

1-2014

Dynamic analysis of DNA nanoparticle immobilization to model biomaterial substrates using combinatorial spectroscopic ellipsometry and quartz crystal microbalance with dissipation

Tadas Kasputis

University of Nebraska-Lincoln, s-tkasput1@unl.edu

Alex Pieper

University of Nebraska-Lincoln


Mathias Schubert

University of Nebraska-Lincoln, mschubert4@unl.edu

Angela K. Pannier

University of Nebraska-Lincoln, apannier2@unl.edu

Follow this and additional works at: <https://digitalcommons.unl.edu/biosysengfacpub>

 Part of the [Bioresource and Agricultural Engineering Commons](#), [Condensed Matter Physics Commons](#), [Environmental Engineering Commons](#), and the [Other Civil and Environmental Engineering Commons](#)

Kasputis, Tadas; Pieper, Alex; Schubert, Mathias; and Pannier, Angela K., "Dynamic analysis of DNA nanoparticle immobilization to model biomaterial substrates using combinatorial spectroscopic ellipsometry and quartz crystal microbalance with dissipation" (2014). *Biological Systems Engineering: Papers and Publications*. 438.

<https://digitalcommons.unl.edu/biosysengfacpub/438>

This Article is brought to you for free and open access by the Biological Systems Engineering at DigitalCommons@University of Nebraska - Lincoln. It has been accepted for inclusion in Biological Systems Engineering: Papers and Publications by an authorized administrator of DigitalCommons@University of Nebraska - Lincoln.

Dynamic analysis of DNA nanoparticle immobilization to model biomaterial substrates using combinatorial spectroscopic ellipsometry and quartz crystal microbalance with dissipation

Tadas Kasputis,^{1,4} Alex Pieper,^{1,4} Mathias Schubert,^{2,3,4} and Angela K. Pannier^{1,3,4}

1 Department of Biological Systems Engineering, University of Nebraska–Lincoln, Lincoln, NE 68588

2 Department of Electrical Engineering, University of Nebraska–Lincoln, Lincoln, NE 68588

3 Nebraska Center for Materials and Nanoscience, University of Nebraska–Lincoln, Lincoln, NE 68588

4 Center for Nanohybrid Functional Materials, University of Nebraska–Lincoln, Lincoln, NE 68588

Corresponding author — A.K. Pannier, University of Nebraska–Lincoln, Department of Biological Systems Engineering, 231 LW Chase Hall Lincoln, NE 68583-0726, USA; tel 402-472-0896, fax 402-472-6338; email apannier2@unl.edu

Abstract

Gene expression within cells can be altered through gene delivery approaches, which have tremendous potential for gene therapy, tissue engineering, and diagnostics. Substrate-mediated gene delivery describes the delivery of plasmid DNA or DNA complexed with nonviral vectors to cells from a surface, with the DNA immobilized to a substrate through specific or nonspecific interactions. In this work, DNA-nanoparticle (DNA–NP) adsorption to substrates is evaluated using combinatorial, *in situ* spectroscopic ellipsometry and quartz crystal microbalance with dissipation (SE/QCM-D), to evaluate the basic dynamic processes involved in the adsorption and immobilization of DNA–NP complexes to substrates. The concentration of DNA–NP solutions influences the adsorbed DNA–NP surface mass, which increases by a factor of approximately 6 (detected by SE) and approximately 4.5-fold (detected by QCM-D), as the DNA concentration increases from 1.5 $\mu\text{g/mL}$ to 15 $\mu\text{g/mL}$, with an increase in layer porosity. In addition, SE/QCM-D analysis indicates that DNA–NP adsorption rates, surface coverage densities, and volume fractions are dependent on the type of substrate: gold (Au) and silicon dioxide substrates, protein-coated and uncoated substrates, and surfaces modified with alkanethiol self assembled monolayers (SAMs). These studies also demonstrate that the influence of an adsorbed protein layer on resulting DNA–NP immobilization efficiency is substrate dependent. For example, Au surfaces coated with fetal bovine serum (FBS) resulted in two-fold greater mass of adsorbed DNA–NPs, compared to DNA–NP adsorption to FBS-coated SAM substrates. This investigation offers insights into dynamic DNA–NP surface adsorption processes, characteristics of the immobilized DNA–NP layer, and demonstrates substrate-dependent DNA–NP adsorption.

Keywords: Spectroscopic ellipsometry, Quartz crystal microbalance with dissipation, DNA nanoparticles, Nonviral gene delivery, Adsorption, Surface immobilization

1. Introduction

Gene delivery approaches serve to introduce exogenous genetic material into cells and find a wide variety of uses in biotechnology, therapeutics, tissue engineering, molecular biology, and high-throughput analytical processes [1,2]. Nonviral gene delivery approaches differ from the use of viral vectors in that they not only are less toxic, less immunogenic, and less costly to produce, but also suffer from being less efficient in gene delivery [3,4]. Nonviral gene complexes typically consist of circular, plasmid DNA, which is highly negatively charged, electrostatically complexed with cationic lipids or polymers to form lipoplex and polyplex DNA–nanoparticles (DNA–NPs), respectively [4–6]. There have been many efforts to increase the efficiency of nonviral complex delivery, including alternative delivery strategies like substrate-mediated gene delivery (SMD). SMD is a technique where DNA–NPs are immobilized to substrates, and cells are then seeded onto these DNA–NPs [7–10]. SMD is often compared and contrasted to bolus gene delivery, a more traditional gene delivery technique where DNA–NP

complexes are simply pipetted into cell culture media and allowed to diffuse to the seeded cell layer. In comparison to bolus methods, SMD is a particularly advantageous gene delivery technique, as immobilization of DNA to surfaces places it directly within the cell's microenvironment, therefore overcoming diffusion and mass transport limitations associated with trafficking of nonviral complexes to cells [9]. In addition, the immobilization of DNA complexes to a substrate enhances gene transfer, since surface immobilization of DNA–NPs has the ability to preserve NP size observed in solution and inhibit complex aggregation, while cytotoxicity is reduced because less DNA is required to achieve gene transfer [7–9,11–13]. Finally, SMD offers the ability to pattern the immobilization of nonviral complexes on surfaces, which can lead to patterned transgene expression, which is particularly pertinent to tissue engineering applications [7].

For SMD, the properties of the surface are critical to both immobilization strategies and transfection (gene transfer) efficiencies. For example, previous work has investigated surface chemistry as a variable to improve SMD, employing self assembled monolayers

(SAMs) of alkanethiols on gold to influence electrostatic interactions between the surface and DNA–NP complex [7,8]. In addition, the roles of nonspecific interactions in DNA–NP adsorption and enhanced transfection have been investigated on surfaces coated with extracellular matrix and serum proteins, such as fetal bovine serum (FBS) [9,11]. However, existing SMD studies focus primarily on substrate biocompatibility and the effectiveness of cellular transgene expression, where the dynamic processes involved in DNA–NP adsorption to substrates have not yet been thoroughly evaluated. Therefore, the objective of this study was to employ a combinatorial analytical approach—in situ spectroscopic ellipsometry and quartz crystal microbalance with dissipation (SE/QCM-D), to evaluate DNA–NP adsorption to various model biomaterial substrates, as well as to examine the influence of DNA–NP concentration on substrate immobilization efficiencies.

While both SE and QCM-D are commonly used separately, only recently have these devices and techniques been combined to form a hybrid measurement platform known as combinatorial in situ SE/QCM-D, which is used to characterize the adsorption processes of a diverse array of organic molecules and thin films [14–19]. By combining both measurement systems, new physical parameters of thin films can be elucidated, such as the porosity of a thin film or the amount of entrapped and associated solvent in real time. Spectroscopic ellipsometry (SE) is a noninvasive surface characterization technique that employs a probing polarized light beam, which upon interacting with the surface, is transmitted through and/or reflected off of the sample into the SE detector [20]. The change in the polarization of light is reported as the complex reflectance ratio values Ψ and Δ , which are subsequently modeled to provide information regarding the physical and magneto-optic properties of thin films, upon consideration of various factors, such as material optical constants and dielectric functions. In situ ellipsometry refers to the repeated acquisition of SE measurements over the course of specified time points, in which various properties (i.e. degradation or doping) of thin films can be monitored over time in either dry or liquid ambient environments. Quartz crystal microbalance with dissipation (QCM-D) is an acoustical measurement technique that operates on the principles of piezoelectric nanogravimetry, allowing for the in situ acquisition of thin film and molecular adsorbate physical parameters, such as thickness, surface coverage density, and viscoelasticity [21,22]. The QCM-D unit triggers shear vibration waves in a pulse mode, and changes in frequency, indicative of surface adsorption of molecular rearrangement on the sensor surface, are detected between the wave pulse time points. Rate measurements of pulsed signal decay, commonly known as dissipation, allow for the evaluation of adsorbate viscoelastic properties. In the combinatorial system, the QCMD sensor provides an interface for studying surface interactions and is mounted within an airtight liquid flow cell, which contains windows for the SE light beam to also probe the QCM-D sensor. Detailed accounts of in situ combinatorial SE/QCM-D experimental and theoretical principles are presented in previously published literature [14,18]. SE/QCM-D can be used as a quick, reliable, and noninvasive tool to accurately monitor adsorption processes and to standardize or optimize substrate immobilization strategies. Previous investigations of DNA–NP immobilization to substrates have only focused on measurements of radiolabeled DNA complexes, without access to parameters that are measured in situ by SE/QCM-D, such as adsorption mass, kinetics, and porosity. In this work, combinatorial in situ SE/QCM-D was employed to probe dynamic adsorption processes of DNA–NPs to various model biomaterial substrates, allowing for the ability to measure DNA–NP physical adsorption characteristics that are influenced by either DNA–NP concentration or substrate composition. Thorough evaluation of DNA–NP adsorption processes to model biomaterial substrates is necessary to better understand SMD from the perspective of the physical properties of the DNA–NP/biomaterial interface, and to further improve SMD through surface engineering and DNA–NP optimization strategies.

2. Materials & methods

2.1. Substrate preparation

Gold (Au) and silicon dioxide (SiO_2) QCM-D sensors were used for all DNA–NP adsorption studies (Q-sense, Linthicum Heights, MD). Prior to beginning in situ SE/QCM-D measurements, ex situ SE measurements of the substrates were obtained to fit optical constants of the substrate without the liquid cell (in ambient air), with the liquid cell to account for window effects by fitting an angle offset and delta offsets (in ambient air), as well as fitting substrate optical constants with buffer in the flow cell. This procedure is described in greater detail elsewhere [14]. For studies involving SAMs on Au, SAMs were prepared on fresh gold QCM-D sensors by first cleaning the substrate with acetone and 200 proof sterile-filtered, degassed ethanol, then immersing the sensor in 5 mL of 2.00 mM alkanethiol. Following 45 min of immersion in thiol solution, QCM-D sensors were removed, rinsed with 200 proof ethanol, and dried with a stream of nitrogen gas. SAM formation was confirmed with ex situ spectroscopic ellipsometry as well as contact angle (data not shown). For studies involving FBS-coated surfaces, substrates were coated with 10% FBS solution (dissolved in 1× tris-buffered saline) during an in situ SE/QCM-D measurement and further details on this substrate coating step can be found in Section 2.3.

2.2. Solution preparation

Tris-buffered saline (TBS) was prepared in a 1× dilution by combining 100 mM tris(hydroxymethyl)aminomethane, pH = 7.2; 150 mM NaCl, and sterile-filtered nanopure H_2O . The 1× TBS buffer was used as the running buffer for dynamic SE/QCM-D measurements, rinsing following DNA–NP adsorption, as well as the buffer used to prepare DNA–NPs. DNA–NPs were prepared through electrostatic complexation by combining plasmid DNA pEGFP-LUC, which encodes for both the enhanced green fluorescent protein (EGFP) and firefly luciferase protein (LUC) under the direction of a cytomegalovirus (CMV) promoter, and 25 kDa branched polyethylenimine (PEI—Sigma-Aldrich, St. Louis, MO, nitrogen:phosphate ratio of 20 in 1× TBS). This nitrogen:phosphate ratio used to prepare the complexes yields DNA–NPs that consist of approximately 27% mass DNA, while the remaining mass fraction of the formulation consists of PEI. For a control study involving the adsorption of uncomplexed PEI, 2 mL of PEI solution was prepared at a concentration of 41 $\mu\text{g}/\text{mL}$, which is the same concentration of PEI used when complexing with 15 $\mu\text{g}/\text{mL}$ to form DNA–NPs used for most studies. For studies involving SAMs on Au, fresh 2.00 mM solutions of 8-mercaptooctanoic acid (Sigma-Aldrich) were prepared in sterile-filtered, nitrogen degassed, 200 proof ethanol. FBS protein solution was prepared by diluting 100% heat-inactivated FBS (Life Technologies, Carlsbad, CA) to 10% in 1× TBS.

2.3. Combinatorial SE/QCM-D measurements

DNA–NP immobilization to SiO_2 , Au, and SAM substrates was monitored in real-time using combinatorial SE/QCM-D. Detailed accounts of SE/QCM-D data acquisition and modeling can be found in previously published work [14,18]. Briefly, the combinatorial SE/QCM-D setup consists of an E1 QCM-D module (Q-Sense, Linthicum, MD) mounted to the sample stage of a M-2000 spectroscopic ellipsometer (J.A. Woollam, Co., Lincoln, NE), set at an angle of incidence 65° relative to the substrate normal. The QCM sensor is placed into a sealed chamber, which is subsequently mounted onto the E1 module. Throughout the course of the measurement, SE detects changes in optical polarization of psi and delta, which was modeled using a Cauchy top-layer, assuming an index of refraction $n=1.5$ and extinction coefficient $k=0$, while the liquid ambient (1× TBS) was assumed to have the same optical constants as water [14,15,17]. QCM-D detects changes in frequency and dissipation of pulse-mode induced shear vibrations of the QCM-D sensor.

The Sauerbrey relation was used to calculate the adsorbed mass detected by QCM-D via changes in frequency upon biomolecule adsorption, since the layer of DNA-NPs on the surface was assumed to be a rigid, solid film [14,16–18]. Additionally, for SE/QCM-D data modeling, which is covered in detail in another publication [14], the densities for both the ambient medium (1× TBS) and the organic medium (DNA-NP solution prepared in 1× TBS) were assumed to be 1, since specific gravity data is not available for these solutions. Flow of liquid medium was facilitated by means of chemical resistant Tygon brand polyurethane tubing (U.S. Plastic Corp, Lima, OH), connected to a flow pump (flow rate = 0.1 mL/min) (New Era Pump Systems, Farmingdale, NY). Tris-buffered saline (1× TBS), a common salt-buffer used for preparing DNA-NPs, was flowed into the liquid chamber and both instruments were allowed to baseline due to routine perturbations upon data acquisition initialization. For studies involving an FBS protein coating, 10% FBS was introduced into the flow cell and allowed to flow over the surface for 90 min, followed by a 30 min 1× TBS rinse. DNA-NP solutions were prepared as described above and allowed to complex for a total of 20 min. DNA-NP solution was allowed to flow over the surface for 20 min with a flow rate of 0.1 mL/min (2 mL total volume), then flow was stopped to allow the DNA-NPs to adsorb to the surface for approximately 90 min, similar to previously reported DNA-NP immobilization timeframes [7,8]. 1× TBS rinse buffer was then flowed into the liquid flow cell at a rate of 0.1 mL/min for 30 min to rinse away any passively associated DNA-NPs.

3. Results & discussion

Surface immobilization of DNA-NPs has previously been shown to enhance nonviral delivery to cells when compared to the bolus delivery approach [9], presumably due to an increased concentration of DNA-NPs immobilized directly within the cells' microenvironment [7,9,23]. For SMD, the properties of the surface are critical to immobilization strategies and transfection (gene transfer) efficiencies. While existing SMD studies focus primarily on substrate biocompatibility and the effectiveness of cellular transgene expression, the dynamic processes involved in DNA-NP adsorption to substrates have not yet been thoroughly evaluated. In this study, combinatorial in situ SE/QCM-D was used to investigate DNA-NP concentration and model biomaterial substrate influences on DNA-NP immobilization kinetics, mass, and porosity. Combinatorial SE/QCM-D was used for this investigation since both SE and QCM-D can measure adsorption masses in situ (i.e. real-time), though the adsorbed mass measured by SE is a measure of the mass of only organic constituents of the thin film, while QCM-D measures the adsorbed mass of the organic constituents including entrapped and associated solvent molecules [14,18]. Therefore, any differences reported in SE and QCM-D adsorbed mass for a given treatment do not indicate conflicting measurement results, but rather demonstrate the different components being measured by the two different instruments. These distinctions between the two different measurements allow access to additional parameters, such as the volume fraction, which can quantitatively describe the porosity of thin films [14–18]. Decreasing volume fractions indicate increasing porosity (i.e. more ambient inclusions) and vice versa, and can be quantitatively represented as a percentage between 0% (no organic component, simply ambient solvent) and 100% (all organic component with no ambient inclusions). In this study, the influence of DNA-NP solution concentration on DNA-NP substrate immobilization properties was evaluated, followed by a detailed analysis of DNA-NP immobilization to various substrates using an optimal DNA-NP solution concentration. Au and SiO₂ substrates were selected for this study since these surfaces are biocompatible, can be easily modified (for example, with SAMs), and have been used previously for evaluating surface adsorption of various peptides [24,25], DNA probes [26], as well as for DNA-NP SMD investigations [7,8]. The immobilization of a FBS protein layer to the substrate prior to DNA-NP immobilization was also evaluated since previous investigations found that FBS immobilization can

enhance SMD of DNA [7,9], although the mechanisms of this enhancement were not evaluated.

3.1. DNA-NP concentration influences DNA immobilization efficiency

The influence of DNA-NP solution concentration on substrate immobilization efficiency to Au is demonstrated by the combined SE/QCM-D plots shown in Figure 1. Changes in adsorbed mass and porosity following DNA-NP adsorption are reported (Table 1) as an average and associated standard error of the final 30 data-points of each measurement (following DNA-NP adsorption and subsequent TBS rinsing). The in situ SE measurements indicate that the final mass (after rinsing with TBS) of immobilized DNA-NPs increases as a function of concentration between the 1.5 µg/mL (Figure 1A) and 15 µg/mL (Figure 1B) conditions (Table 1). Similar to SE trends, QCM-D measurements indicate a trend of increasing adsorbed DNA-NP mass with increasing DNA-NP solution concentrations (Table 1, Figure 1). A control study (data not shown) was conducted to examine the adsorption of uncomplexed PEI to Au (not coated with FBS), which showed that for free PEI (i.e. not complexed with DNA), the mass detected for PEI adsorption to Au by SE is 24% of the adsorbed mass of DNA-NPs to Au, while the PEI mass detected by QCM-D is only 9% of the measured DNA-NP mass on Au (Figure 1B). In addition, the adsorption rate of uncomplexed PEI to gold is extremely fast, as maximal adsorption of free PEI to gold is observed within 5–10 min of PEI introduction to the measurement apparatus (data not shown). This comparison demonstrates that if free PEI was present in the DNA-NP solution, this uncomplexed PEI would represent a very small fraction of materials bound to the substrate.

While the two instruments detected different absolute amounts of adsorbed DNA-NP mass, that reported by SE is a measure of the mass of organic constituents of the thin film, while the QCM-D measurements also account for the entrapped and associated solvent molecules of the organic constituents [14,18]. Thus, the differences between the two different measurements allow access to additional parameters, such as the volume fraction, which can quantitatively describe the porosity of thin films [14–18]. The volume fraction was found to increase slightly between the 1.5 µg/mL and 15 µg/mL DNA-NP conditions (Table 1), which suggests improved DNA-NP packing as the mass of immobilized DNA-NPs increase, as indicated by the DNA-NP adsorption masses obtained by SE and QCM-D. These findings are important in optimizing SMD systems, since for optimal transfection, DNA-NPs not only must be immobilized to the substrate, but also retain the ability to be displaced so that complexes can be easily endocytosed by cells for efficient DNA delivery to cells.

These combined measurements of detecting “dry” mass (organic component) and “wet” mass (organic component with ambient inclusions), have not previously been conducted for DNA-NP adsorption to surfaces and the correlations reported here differ from previous studies. For example, Bengali et al. [9], reported that increasing concentrations of DNA-PEI NPs added to FBS-coated polystyrene surfaces did not influence the adsorbed mass of DNA, an observation that contradicts the trend from the SE/QCM-D results shown in Figure 1. However, SE/QCM-D provides a more precise perspective of DNA-NPs associated with a surface, since loosely bound, passively adsorbed DNA-NPs are also evaluated with SE/QCM-D. For previously reported radioactivity measurements, loosely bound DNA-NPs would have been washed off the surface during rinse steps before even conducting admeasurement, thus measuring only tightly bound DNA-NPs, which explains why QCM-D detects an increased mass of adsorbed and loosely associated DNA-NPs relative to previous studies [7–9,11]. Another important difference to note is that previous DNA radiolabeling studies reported the adsorbed mass of DNA instead of the entire DNA-NP complex since DNA was the labeled component that was measured. Therefore, the measurements reported here represent a more accurate representation of in situ DNA-NP substrate immobilization.

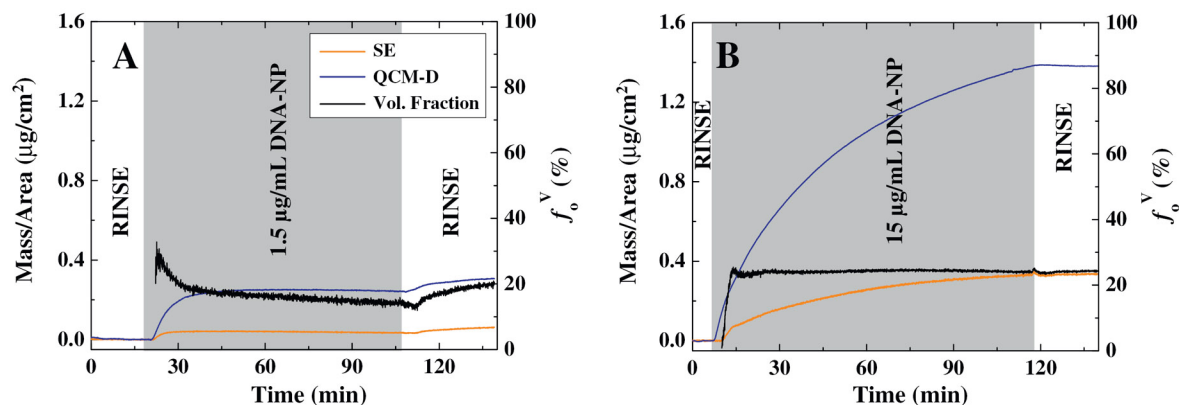


Figure 1. DNA–NP solution concentrations influence DNA–NP surface coverage and layer packing. Combined SE/QCM-D plots are shown below depicting the modeled SE (orange line) and QCM-D (blue line) mass/area parameters, reported in $\mu\text{g}/\text{cm}^2$ on the left y-axis, as well as the volume fraction (black line), reported as a percentage on the right y-axis for DNA–NP adsorption to Au at DNA concentrations of 1.5 $\mu\text{g}/\text{mL}$ (A) and 15 $\mu\text{g}/\text{mL}$ (B), with a constant N/P ratio = 20 for complexation with PEL.

Table 1. Influence of DNA–NP concentration on complex immobilization to Au substrates.

	Δ_{SE} ($\mu\text{g}/\text{cm}^2$)	$\Delta_{\text{QCM-D}}$ ($\mu\text{g}/\text{cm}^2$)	$\Delta_{\text{vol. fraction}}$ (%)
1.5 μg DNA	0.0611 ± 0.0003	0.3071 ± 0.0002	19.92 ± 0.10
15 μg DNA	0.3406 ± 0.0005	1.3828 ± 0.0001	24.63 ± 0.03

Finally, SE/QCM-D allowed for measurements of DNA–NP adsorption as it occurred in real-time (i.e. in situ). The rate of DNA–NP adsorption was found to decrease with increasing DNA concentration, as more time was required for DNA–NP adsorbing mass to plateau as indicated by the SE/QCM-D plots presented in Figure 1. The observation of decrease in adsorption rate with increasing DNA–NP concentration, combined with the increasing porosity observation, suggests that solvent–particle interactions (i.e. aggregation of DNA–NPs in solvent) become increasingly pronounced at high DNA–NP concentrations, which is also documented in previous literature regarding polyplex and lipoplex DNA–NPs [27–29]. In summary, this study demonstrates that DNA–NP concentration influences adsorbate mass, porosity, and the rate of adsorption of immobilized DNA–NPs. The access to previously unattainable surface properties, in particular the volume fraction, allows for a deeper understanding of the conformation and stability of immobilized DNA–NPs, which could be used to develop more efficient SMD systems for nonviral gene delivery.

3.2. Substrates influence dynamic immobilization properties of DNA–NP thin films

Previous studies on substrate immobilization of DNA–NPs for SMD found that coating substrates with either extracellular matrix proteins or mixtures of serum proteins found in FBS can increase DNA–NP immobilization to polystyrene surfaces, and also increases the efficiency of DNA–NP delivery to cells [9,11]. In addition, studies have demonstrated that surface charge and presence of PEG groups on surfaces enhance DNA–NP immobilization and nonviral SMD of genes to cells [8]. This investigation focuses on elucidating the dynamics of DNA–NP immobilization processes and substrate–material interactions, including adsorption rate, adsorption mass, and porosity, as a function of surface material, surface charge, and protein coatings. Triplicate SE/QCM-D measurements were acquired to ensure measurement reproducibility for each substrate condition evaluated (Au, SiO_2 , and SAMs), both with and without FBS protein coatings using the optimal DNA–NP solution concentration (15 $\mu\text{g}/\text{mL}$ DNA; N/P=20) determined in Section 3.1. A comprehensive summary of changes in adsorbed mass and volume fraction is reported in Table 2 for these measurements. The values presented in Table 2 were obtained by calculating the difference in adsorbed DNA–NPs upon rinsing with

TBS, relative to the rinse phase immediately preceding DNA adsorption. A total of 30 data-points were analyzed per replicate and pooled with their respective replicate measurements for a total of 90 data points, from which average mass/area or volume fraction percentage and corresponding standard error values are reported. In addition, Figure 2 contains representative in situ SE/QCM-D measurement plots for DNA–NP adsorption to various model biomaterial substrates.

For DNA–NP immobilization to a SiO_2 substrate (Figure 2A), SE initially detected a very small quantity of DNA–NP adsorption, which further decreased upon rinsing with TBS to yield an adsorbed mass of $0.017 \pm 0.002 \mu\text{g}/\text{cm}^2$, while QCM-D detected a steadily increasing quantity of DNA–NP adsorption to SiO_2 , which leveled out to approximately $0.877 \pm 0.037 \mu\text{g}/\text{cm}^2$ upon rinsing with TBS following the DNA–NP adsorption phase (Table 1). For a SiO_2 substrate coated with a FBS protein layer (Figure 2C), SE indicates that the adsorbed mass of DNA–NPs doubles with respect to DNA–NP adsorption to SiO_2 without FBS, while the adsorbed mass detected by QCM-D remains similar compared to DNA–NP adsorption to SiO_2 without FBS (Table 1). Although the changes in volume fractions reported in Table 1 indicate very slight changes in volume fraction over the course of the DNA–NP adsorption itself, the total volume fraction was increased in the case of SiO_2 + FBS, as seen in Figure 2 (A and C). These measurements indicate that SiO_2 + FBS enhances DNA–NP adsorption when compared to DNA–NP adsorption to SiO_2 . Examination of the total volume fraction indicates that DNA–NPs on SiO_2 + FBS form a more packed layer (in conjunction with the FBS coating) than on uncoated SiO_2 , as indicated by the approximate total 37% volume fraction of DNA–NPs on SiO_2 + FBS, and steadily decreasing volume fraction of DNA–NPs on bare SiO_2 as seen in Figure 2 (A and C). These results demonstrate that DNA–NPs barely adsorb to unmodified SiO_2 substrates and instead require an adsorbed protein coating to facilitate DNA–NP substrate immobilization to SiO_2 . This observation concurs with previous findings regarding the adsorption of biomolecules to SiO_2 , in which biomolecule adsorption to SiO_2 is inhibited compared to other surfaces, such as Au [24]. Biofunctionalization (i.e. streptavidin–biotin system) of SiO_2 surfaces is commonly required to enhance the binding of biomolecules by modifying the SiO_2 surface with components that will bind biomolecules [30,31].

When DNA–NPs were immobilized to an unmodified Au substrate (Figure 2B), both SE and QCM-D indicated notable increases

Table 2. Comprehensive summary of DNA–NP adsorption to various model biomaterial surfaces.

	Δ_{SE} ($\mu\text{g}/\text{cm}^2$)	Δ_{QCM-D} ($\mu\text{g}/\text{cm}^2$)	$\Delta_{vol. fraction}$ (%)
SiO ₂	0.017 ± 0.002	0.877 ± 0.037	1.497 ± 0.144
SiO ₂ + FBS	0.038 ± 0.010	0.833 ± 0.044	-2.609 ± 0.656
Au	0.265 ± 0.007	1.207 ± 0.014	21.84 ± 0.46
Au + FBS	0.226 ± 0.001	0.863 ± 0.026	-5.434 ± 0.456
SAM	0.141 ± 0.009	1.694 ± 0.031	7.708 ± 0.411
SAM + FBS	0.130 ± 0.016	0.539 ± 0.022	0.730 ± 0.383

in adsorbed mass and volume fraction (Table 2) relative to the unmodified SiO₂ substrate (Figure 2A). These measurements confirm that DNA–NPs can adsorb to unmodified substrates without FBS, in contrast to DNA–NP adsorption to SiO₂ substrates. Interestingly, upon DNA–NP adsorption to FBS coated Au (Au + FBS), both SE and QCM-D detected less adsorbed mass of DNA–NPs relative to unmodified Au substrates (Table 1). In addition, although the relative volume fractions reported for both Au and Au + FBS decrease upon DNA–NP immobilization, the total volume fraction of the combined FBS and DNA–NP layer is approximately 10% greater than the volume fraction following DNA–NP adsorption to Au (Figure 2B and D). The observed differences in the volume fractions indicate that the total degree of molecular packing of the FBS and DNA–NP layer on Au is greater than DNA–NPs on Au, which suggests that DNA–NPs are engaged in nonspecific binding interactions with the adsorbed protein. Additionally, the amount of immobilized DNA–NPs detected by SE (dry, organic component) is comparable to the amount of immobilized DNA–NPs detected in previous investigations. For example, measurements of radiolabeled DNA by Bengali et al., reported between 0.1 and 0.3 $\mu\text{g}/\text{cm}^2$ of adsorbed DNA–PEI complexes after 2 h to polystyrene and FBS-coated polystyrene [9], while measurements of radiolabeled DNA by Pannier et al., reported between 0.3 and 0.5 $\mu\text{g}/\text{cm}^2$ of adsorbed DNA–PEI complexes to SAM surfaces formed with mixtures of alkanethiols including some with PEG terminal functional groups [8]. In summary, the investigations of DNA–NP adsorption to Au reveal that DNA–NPs can adsorb to both Au and Au + FBS surfaces with increased quantities of immobilized DNA–NPs compared to DNA–NP adsorption to SiO₂ and SiO₂ + FBS substrates, respectively. These findings indicate that different types of substrates influence DNA–NP adsorption and immobilization characteristics.

Hydrophilic carboxyl-terminated SAM modifications to gold were investigated, since this simple chemical surface modification has previously been shown to influence DNA–NP immobilization and resulting SMD transfection characteristics [7]. Interestingly, SE indicated that less DNA–NP is adsorbed to SAMs than to Au, while QCM-D indicates increased DNA–NP adsorption to SAMs relative to Au substrates (Table 2). The SE measurements suggest that while less DNA–NPs may be immobilized to the SAMs relative to Au, the QCM-D measurements indicate that more DNA–NPs are loosely associated with the SAM surface when compared to DNA–NPs on Au. Therefore, while the SE comparison mentioned above contradicts previously published trends, the QCM-D data suggests that SAM surfaces loosely bind DNA–NPs, which could be more easily endocytosed by cells within the local microenvironment, possibly explaining the increased transfection efficiency reported when DNA–NPs are immobilized to SAMs [7]. DNA–NP adsorption mass to carboxyl-terminated SAMs (Figure 2C) was increased (Table 2) on SAMs without a FBS coating relative to SAMs with FBS (Figure 2F), concurrent with the DNA–NP adsorption trends between unmodified and FBS-coated Au and SiO₂ surfaces. Additionally, the relative change in volume fraction increased upon DNA–NP adsorption to uncoated SAMs, while the volume fraction did not significantly change upon DNA–NP adsorption to SAM + FBS substrates (Table 2), which indicates that DNA–NPs form a more densely packed layer on the SAMs without an FBS coating. This trend of differing volume fractions between uncoated and FBS-coated substrates is

consistent with the volume fraction trends demonstrated on SiO₂ and Au surfaces. This trend suggests that increased DNA–NP volume fractions on uncoated substrates relative to their FBS-coated counterparts is demonstrating a more pronounced change in molecular packing, since measurements of DNA–NP adsorption to uncoated substrates begin with no molecules (i.e. FBS) on the surface, instead of measuring the change in volume fraction between surfaces already coated with molecules (FBS) and DNA–NPs adsorbed to FBS. In other words, DNA–NPs adsorbing to FBS-coated substrates are adsorbing to a packed layer of protein molecules and may simply replace or re-arrange the existing FBS layer, thereby causing minor changes in molecular packing, which can complicate the measurement of adsorbed DNA–NP mass to FBS coated substrates.

For the different surfaces coated with FBS (Figure 2B, D, E), the FBS adsorbed mass and porosity to all three surfaces was similar as indicated by SE (approx. 0.3–0.4 $\mu\text{g}/\text{cm}^2$), QCM-D (approx. 0.8–1.0 $\mu\text{g}/\text{cm}^2$), and volume fractions (35–45%). In addition, when analyzing the influence of FBS protein coatings on substrate immobilization of DNA–NPs, the SE/QCM-D data suggest that DNA–NP immobilization efficiency is substrate dependent, since different DNA–NP immobilization trends are observed between different substrates coated with FBS (Table 2). The two previous observations, together, suggest that although similar amounts of protein are adsorbing to the substrate with similar packing characteristics, different proteins within the FBS mixture, including different protein functional groups and binding motifs for DNA–NPs, could be presented on different substrates, as indicated by differences in detected DNA–NP quantities and porosities between the three substrates, as well as reported differences in transfection efficiencies [9,11,32]. Previous work regarding fibronectin protein adsorption to different SAM surfaces has shown that different surface characteristics, such as charge and hydrophobicity, influences the conformation of adsorbing proteins [33], which could influence subsequent adsorption of biomolecules, such as DNA–NPs, due to the exposure of different protein functional groups between surfaces. For example, a comparison between DNA–NP adsorption to SiO₂ + FBS (Figure 2D) and Au + FBS (Figure 2E) demonstrates the different amounts of DNA–NPs that adsorb to the FBS layers on different underlying substrates (Table 2), although the volume fractions are similar between the two substrates due to the similarity in the ratio of measured SE mass and QCM-D mass for both conditions. This observation indicates that while differing amounts of DNA–NP adsorb to each surface, the molecular packing and porosity characteristics are similar. SE/QCM-D demonstrates the specific DNA–NP adsorption characteristics that are influenced by different substrates and by modifications to those substrates, which is an important consideration when optimizing SMD systems for nonviral gene delivery, since the transfection efficiency relies on DNA–NP loading and release to/from the substrate. Additionally, these SE/QCM-D studies suggest that while FBS may not be increasing the amount of adsorbed DNA to certain substrates, for example Au, FBS may be more important in facilitating favorable cell–material interactions for the endocytosis of immobilized DNA–NPs as suggested by previous studies [11,34]. This investigation demonstrates that SE/QCM-D can be used as a quick, reliable, and noninvasive tool to accurately monitor DNA–NP adsorption processes and to standardize or optimize substrate immobilization strategies in real time. The SE/QCM-D results also demonstrate the need for system optimization when using new substrates and/or solution concentrations to immobilize DNA–NPs.

4. Conclusions

Dynamic processes of DNA–NP immobilization to various substrates were evaluated using in situ combinatorial SE/QCM-D. Analysis of the influences of DNA–NP solution concentration on DNA–NP adsorption demonstrated that increasing DNA–NP concentrations result in increasing mass of adsorbed DNA–NPs, slower rate of adsorption, and increasing volume fraction of resulting DNA–NP films. DNA–NP adsorption to Au, SiO₂, and SAM–Au substrates was evaluated both with and without FBS protein

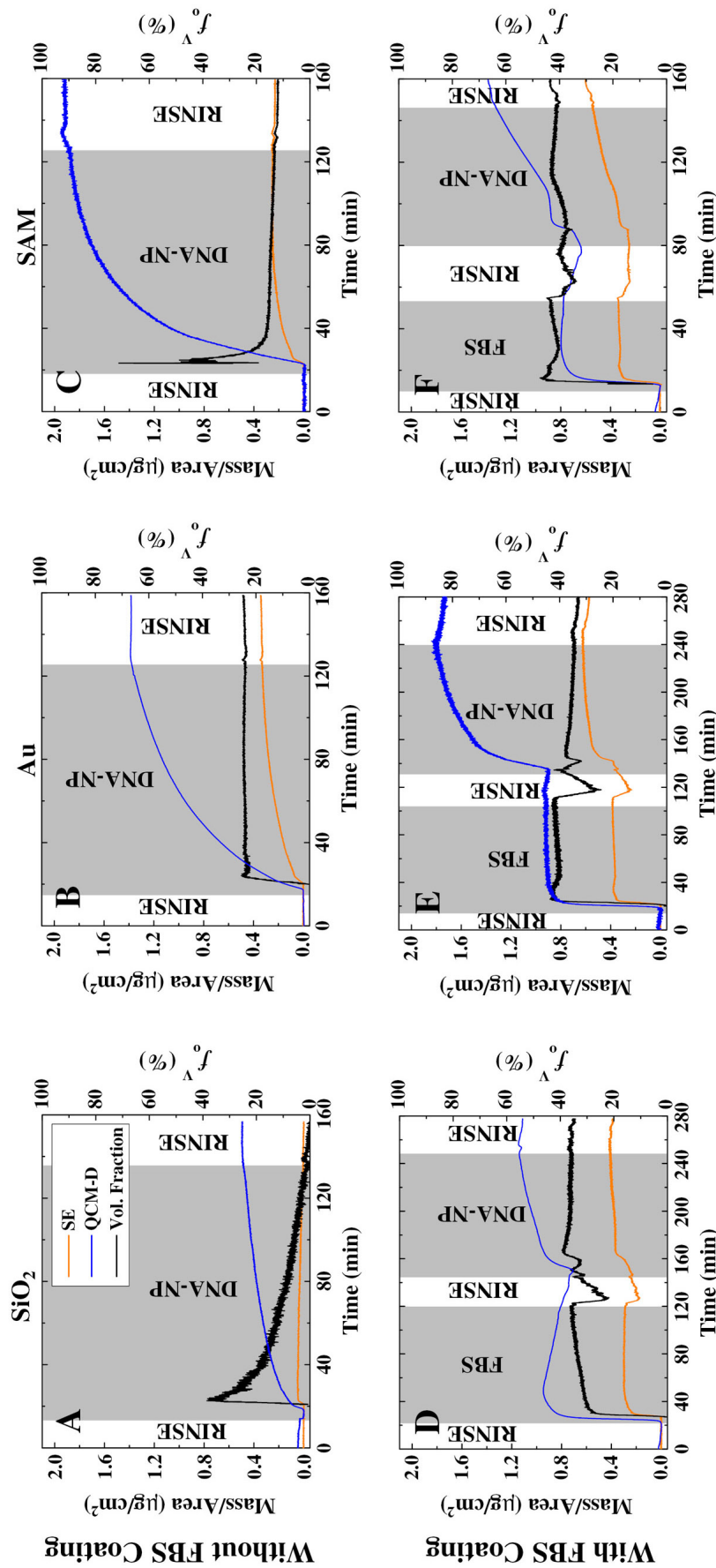


Figure 2. Substrate immobilization of DNA-NP solution to (A) SiO₂, (B) SiO₂ + FBS, (C) Au, (D) Au + FBS, (E) carboxyl-terminated SAM coated with FBS, and (F) carboxyl-terminated SAM coated with FBS. Combined SE/QCM-D plots are shown below depicting the modeled SE (orange line) and QCM-D (black line) mass/area parameters, reported in µg/cm² on the left y-axis, as well as the volume fraction (blue line), reported as a percentage on the right y-axis.

coatings. SE/QCM-D measurements of these various substrates show that DNA–NP adsorption properties, such as adsorbed mass, adsorption rate, and layer porosity, differ between varying surfaces, and that the influence of FBS coatings on DNA–NP adsorption characteristics is substrate dependent. SE/QCM-D can be used as a quick, reliable, and noninvasive tool to accurately monitor adsorption processes and to standardize or optimize various substrate immobilization strategies. While SE and QCM-D are used extensively for quality control and process monitoring in the semiconductor and thin film industries, the biotechnology sector could benefit from this technology for characterizing biological phenomena on the nanoscale, as well as applications including high-throughput screening, lab-on-a-chip, and mass-scale manufacturing process monitoring. Future work is aimed at evaluating DNA–NP loading within porous, uniformly nanostructured thin films using SE/QCM-D, and developing advanced three-dimensional nonviral gene delivery strategies.

Funding sources & acknowledgments — Support for this research was provided in part by funds from the National Science Foundation (CAREER to AKP, CBET-1254415), the Center for Nanohybrid Functional Materials (NSF EPS-1004094), the American Heart Association (#10SDG2640217), the University of Nebraska Foundation (Layman Funds), the J.A. Woollam Company, and the USDA CSREES–Nebraska (NEB-21-146).

References

- [1] A.L. Parker, C. Newman, S. Briggs, L. Seymour, P.J. Sheridan, *Expert Rev. Mol. Med* 5 (2003), doi 10.1017/S1462399403006562.
- [2] M.A. Mintzer, E.E. Simanek, *Chem. Rev.* 109 (2) (2009) 259.
- [3] C.M. Wiethoff, C.R. Middaugh, *J. Pharm. Sci.* 92 (2) (2003) 203.
- [4] S.D. Patil, D.G. Rhodes, D.J. Burgess, *Aaps J.* 7 (1) (2005) E61.
- [5] D. Zhao, T. Gong, D. Zhu, Z.R. Zhang, X. Sun, *Int. J. Pharm.* 413 (1–2) (2011) 260.
- [6] A.K. Pannier, L.D. Shea, *Mol. Ther.* 10 (1) (2004) 19.
- [7] A.K. Pannier, B.C. Anderson, L.D. Shea, *Acta Biomater.* 1 (5) (2005) 511.
- [8] A.K. Pannier, J.A. Wieland, L.D. Shea, *Acta Biomater.* 4 (1) (2008) 26.
- [9] Z. Bengali, A.K. Pannier, T. Segura, B.C. Anderson, J.H. Jang, T.A. Mustoe, L.D. Shea, *Biotechnol. Bioeng.* 90 (3) (2005) 290.
- [10] A.K. Pannier, E.A. Ariazi, A.D. Bellis, Z. Bengali, V.C. Jordan, L.D. Shea, *Biotechnol. Bioeng.* 98 (2) (2007) 486.
- [11] Z. Bengali, J.C. Rea, L.D. Shea, *J. Gene. Med.* 9 (8) (2007) 668.
- [12] T. Segura, L.D. Shea, *Bioconjug. Chem.* 13 (3) (2002) 621.
- [13] T. Segura, M.J. Volk, L.D. Shea, *J. Control. Release* 93 (1) (2003) 69.
- [14] K.B. Rodenhausen, T. Kasputis, A.K. Pannier, J.Y. Gerasimov, R.Y. Lai, M. Solinsky, T.E. Tiwald, H. Wang, A. Sarkar, T. Hofmann, N. Ianno, M. Schubert, *Rev. Sci. Instrum.* 82/10 (2011) 103111.
- [15] T. Kasputis, M. Koenig, D. Schmidt, D. Sekora, K.B. Rodenhausen, K.J. Eichhorn, P. Uhlmann, E. Schubert, A.K. Pannier, M. Schubert, M. Stamm, *J. Phys. Chem. C* 117 (2013) 13971.
- [16] K.B. Rodenhausen, B.A. Duensing, T. Kasputis, A.K. Pannier, T. Hofmann, M. Schubert, T.E. Tiwald, M. Solinsky, M. Wagner, *Thin Solid Films* 519 (9) (2011) 2817.
- [17] K.B. Rodenhausen, D. Schmidt, T. Kasputis, A.K. Pannier, E. Schubert, M. Schubert, *Opt. Express* 20 (5) (2012) 5419.
- [18] K.B. Rodenhausen, M. Schubert, *Thin Solid Films* 519 (9) (2011) 2772.
- [19] E. Bittrich, K.B. Rodenhausen, K.J. Eichhorn, T. Hofmann, M. Schubert, M. Stamm, P. Uhlmann, *Biointerphases* 5 (4) (2010) 159.
- [20] D. Schmidt, C. Müller, T. Hofmann, O. Inganäs, H. Arwin, E. Schubert, M. Schubert, *Thin Solid Films* 519 (9) (2011) 2645.
- [21] J. Benesch, J.F. Mano, R.L. Reis, *Acta Biomater.* 6 (9) (2010) 3499.
- [22] K.A. Marx, *Biomacromolecules* 4 (5) (2003) 1099.
- [23] D. Luo, W.M. Saltzman, *Nat. Biotechnol.* 18 (8) (2000) 893.
- [24] K.P. Fears, D.Y. Petrovykh, T.D. Clark, *Biointerphases* 8 (2013), doi 10.1186/1559-4106-8-20.
- [25] K.P. Fears, T.D. Clark, D.Y. Petrovykh, *J. Am. Chem. Soc.* 135 (40) (2013) 15040.
- [26] H. Kimura-Suda, D.Y. Petrovykh, M.J. Tarlov, L.J. Whitman, *J. Am. Chem. Soc.* 125 (30) (2003) 9014.
- [27] E. Lai, J.H. van Zanten, *Biophys. J.* 80 (2) (2001) 864.
- [28] T.G. Park, J.H. Jeong, S.W. Kim, *Adv. Drug Deliv. Rev.* 58 (4) (2006) 467.
- [29] S.C. De Smedt, J. Demeester, W.E. Hennink, *Pharm. Res.* 17 (2) (2000) 113.
- [30] B. Bhushan, D.R. Tokachichu, M.T. Keener, S.C. Lee, *Acta Biomater.* 1 (3) (2005) 327.
- [31] K.S. Midwood, M.D. Carolus, M.P. Danahy, J.E. Schwarzbauer, J. Schwartz, *Langmuir* 20 (13) (2004) 5501.
- [32] J.H. Jang, Z. Bengali, T.L. Houchin, L.D. Shea, *J. Biomed. Mater. Res.* 77A/1 (2006) 50.
- [33] K.E. Michael, V.N. Vernekar, B.G. Keselowsky, J.C. Meredith, R.A. Latour, A.J. Garcia, *Langmuir* 19 (19) (2003) 8033.
- [34] A. Dhaliwal, M. Maldonado, Z. Han, T. Segura, *Acta Biomater.* 6 (9) (2010) 3436.